The Study of Minor Elements and Shielding Gas on Penetration in TIG Welding of Type 304 Stainless Steel

R.-I. Hsieh, Y.-T. Pan, and H.-Y. Liou

(Submitted 30 March 1998; in revised form 15 September 1998)

The effects of minor elements and shielding gas on the penetration of TIG welding in type 304 stainless steel have been studied. The bead-on-plate test was performed, then the depth and width of the weld were measured using an optical projection machine. The arc voltage was measured with an arc data monitor. In addition, the metallurgical characteristics of weld were examined using OM and SEM. The results show that oxygen and sulfur are beneficial in increasing a depth/width ratio because of the increased surface tension/temperature gradient. Elements, such as aluminum, that have a deleterious effect on the depth/width ratio will combine with oxygen and reduce the soluble oxygen content in the weld pool. On the other hand, silicon and phosphorus have a minor effect on the depth/width ratio. Shielding gas using Ar + 1% O_2 or Ar + 5% H_2 can significantly promote the depth/width ratio. The former contains increased soluble oxygen content in the weld pool, and the latter produces an arc that is hotter than that produced by pure argon.

Keywords depth/width ratio, minor elements, penetration, shield gas, surface tension, TIG welding, type 304 stainless steel, weld pool

1. Introduction

Type 304 stainless steel is extensively used in industry due to its superior low temperature toughness and corrosion resistance. Strips thinner than 3 mm are often processed to form tubes, which are used in the chemical plant for the construction of heat exchangers. In general, the production of type 304 stainless steel tube is carried out in two steps: the continuous forming of strip into tube by rolls and the single-pass of tungsten inert gas (TIG) welding of the seam in the tube. However, variations in weld penetration during the mechanized TIG welding have been reported (Ref 1, 2). This effect is caused by small differences in the composition that alter the flow pattern in the molten weld pool. Recent investigations (Ref 3, 4) have shown that apparently minor changes in sulfur or oxygen content of the metal can result in remarkable variations in weld penetration. Sulfur and oxygen are surface active in iron and cause a substantial decrease in the surface tension, even when they exist in relatively low concentrations. Consequently, small differences in concentration of surface-active elements in the weld pool can account for the variation in welding behavior. On the other hand, levels of surface-active elements in the weld pool are controlled by the presence of scavenging metals, such as aluminum, calcium, and magnesium. Heiple and Roper (Ref 5) propose that the surface tension gradient, $d\gamma/dt$, of the weld pool is altered from a negative to a positive value by the presence of surface-active elements, such as sulfur and oxygen. When the soluble sulfur or oxygen concentration is below a certain critical concentration, the surface tension is highest at the edges of the pool, and the thermocapillary flow occurs radially outward from low to high surface tension and results in a shallow weld (Fig. 1a). However, in oxygen and sulfur concentration above the critical content, surface flow is radially inward, and hot liquid is swept to the bottom of the pool and produces a deeper weld (Fig. 1b). During the development of type 304 stainless steel, variable penetration is also found in the mechanized TIG welding during pipe making. The purpose of

R.-I. Hsieh, Y.-T. Pan, and **H.-Y. Liou,** Steel and Aluminum Research and Development, China Steel Corporation, Taiwan, R.O.C.

Table 1 Chemical compositions of steels used in this study

	Composition, wt%											
Steel	**C**	**Si**	**Mn**	**P**	**S**	**Cr**	**Ni**	**Cu**	**Ti**	**Al**	**N**	**O**
S1	0.036	0.47	1.25	0.0230	0.0028	17.6	8.1	0.25	0.0073	0.0069	0.040	0.0097
S2	0.036	0.47	1.25	0.0230	0.0068	17.6	8.0	0.25	0.0059	0.0060	0.040	0.0064
S3	0.036	0.45	1.22	0.0260	0.0136	17.0	7.8	0.25	0.0072	0.0057	0.038	0.0068
Si1	0.038	0.34	0.74	0.0070	0.0010	18.1	8.5	0.25	0.0089	0.0071	0.046	0.0120
Si2	0.039	0.51	0.75	0.0068	0.0009	18.1	8.5	0.25	0.0087	0.0047	0.046	0.0113
Si3	0.039	0.69	0.74	0.0067	0.0006	18.1	8.5	0.25	0.0085	0.0051	0.046	0.0112
P1	0.036	0.37	0.78	0.0160	0.0013	17.3	8.0	0.25	0.0075	0.0050	0.043	0.0106
P2	0.036	0.37	0.78	0.0260	0.0013	17.3	8.0	0.26	0.0071	0.0051	0.044	0.0098
Al1	0.036	0.35	0.79	0.0230	0.0009	17.7	8.1	0.26	0.0084	0.0062	0.047	0.0095
Al2	0.036	0.35	0.79	0.0240	0.0010	17.7	8.2	0.25	0.0085	0.0090	0.046	0.0064
O1	0.038	0.34	0.74	0.0067	0.0010	18.1	8.5	0.25	0.0090	0.0061	0.046	0.0070
O2	0.036	0.34	0.77	0.0065	0.0010	18.1	8.5	0.25	0.0067	0.0054	0.046	0.0136

this study is to clarify the effect of minor elements of steel and weld shielding gas on the penetration of weld.

2. Experimental Procedure

The experimental steels were prepared from 250 kg vacuum-melted heats and cast into 160 by 160 mm square ingots. Table 1 lists the chemical compositions of the experimental steels. The base composition is 0.03% C-0.78% Mn-18% Cr-8% Ni, and the design is for the variation of sulfur, phosphorus, silicon, aluminum, and oxygen content. The steels were reheated at 1260 °C for two hours and hot rolled to 3.4 mm thick, with finish rolling temperature around 850 °C. Before welding, these steels were subjected to solution treatment at 1100 °C for 10 min and then quenched in cold water. Specimens of dimensions 65 by 350 by 3.4 mm were cut from the strip, and bead-on-plate test welds were performed using TIG arc welding to study the resulting weld depth/width(d/w) ratio. Two different argon-base shielding gases, Ar + 5% H_2 and Ar + 1% O_2, were used to evaluate the effect of shielding gas on the weld d/w ratio. Table 2 shows the welding conditions of TIG for bead-on-plate and butt welding. After welding, about 40 mm of the weld from each end was discarded, and the remainder was cut into five specimens. These specimens were polished and etched with 15 ml HCl + 5 ml NO_3 + 100 ml H_2O solution. Next, the depth and width of weld were measured using an optical projection machine under magnification of 20×. Figure 2 shows the schematic diagram for measuring the width and depth of the weld. In addition, the arc voltage was measured with an arc data monitor that was connected with the output of welder. At the same time, the metallurgical characteristics of the weld, which has markedly variable weld penetrations, were examined using

Table 2 Tungsten inert gas arc welding parameters for bead-on-plate and square butt welds

Parameter	Value
Current, A	150
Travel speed, mm/min	228
Shielding gas(a)	Ar
Backing gas	Ar
Gas flow rate, l/min	15
Arc length, mm	2.0
Electrode size, mm	4.0
Vertex angle, degrees	60
Polarity	DCEN

(a) Only pure argon is used to evaluate the effect of minor elements on the d/w ratio. Ar + 1% O_2 and Ar + 5% H_2 are used to evaluate the effect of shielding gas on the d/w ratio

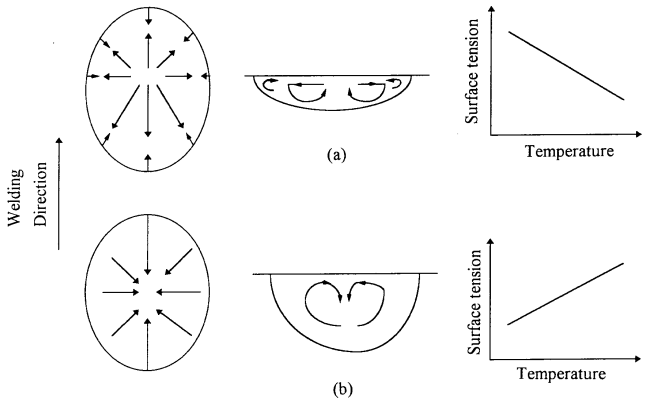

Fig. 1 Fluid flow pattern in weld pool. (a) Negative surface tension gradient. (b) Positive surface tension gradient. Source: Ref 5

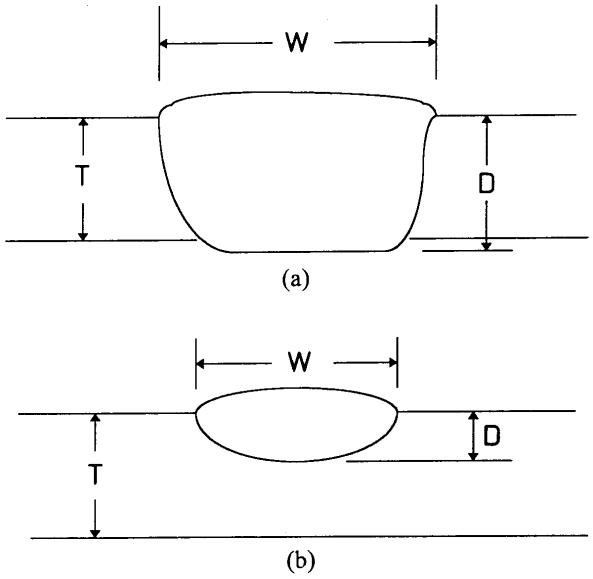

Fig. 2 Schematic for measuring of weld depth and width. (a) Full penetration. (b) Partial penetration

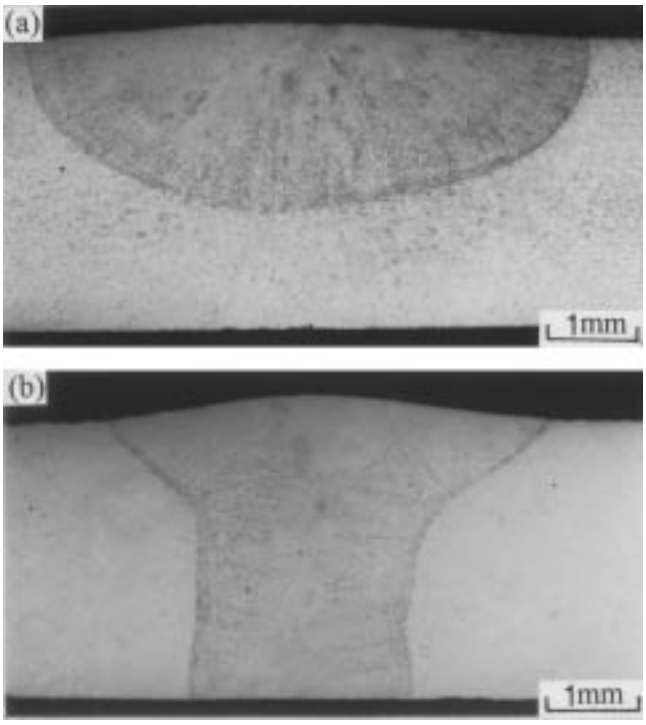

Fig. 3 Macrosection of TIG bead-on-plate weld showing the effect of oxygen content of base metal on the weld geometry. (a) 70 ppm. (b) 120 ppm

an optical microscopy (OM) and scanning electron microscopy equipped with energy dispersive spectrometer (SEM-EDS).

3. Results and Discussion

3.1 The Effect of Minor Elements on the Weld d/w Ratio

Figure 3 shows the macrosection of the TIG bead-on-plate weld at two levels of oxygen content. The oxygen content of the base metal has a significant effect on the weld geometry. A wider and shallower weld can be made at low oxygen contents (Fig. 3a); however, a narrower and deeper weld can be performed at high oxygen contents (Fig. 3b). Figure 4 shows the relationship between the sulfur content of the base metal and the weld *d*/*w* ratio. *The d*/*w* ratio increases with increasing sulfur content. Only half of the thickness was penetrated when the sulfur content was about 30 ppm. However, full penetration can be made when the sulfur content is around 140 ppm. Sulfur is the surface-active element and can combine with iron to form FeS, which is likely to segregate to the surface of the weld pool

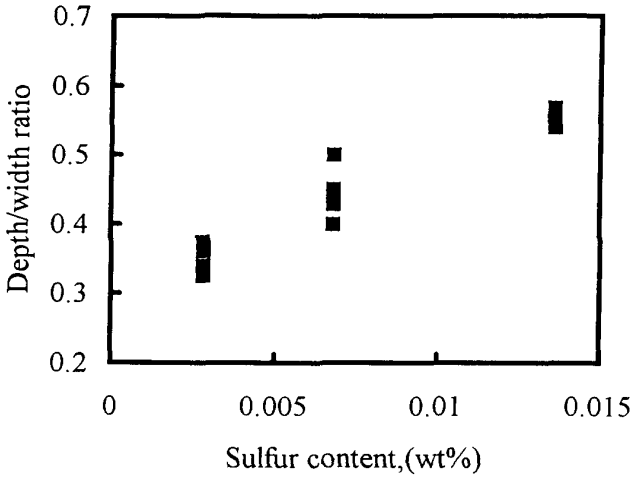

Fig. 4 Relationship between sulfur content of base metal and the weld *d*/*w* ratio

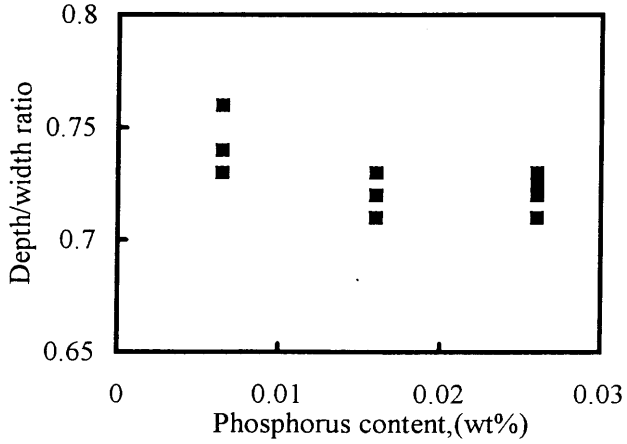

Fig. 5 Effect of phosphorus content of base metal on the weld *d*/*w* ratio

and decrease the surface tension (Ref 6). In addition, the surface tension gradient changes from negative to positive when the soluble sulfur content is above 60 ppm (Ref 4). In this case, the flow of the weld pool is inward; the weld *d*/*w* ratio can be significantly improved. Moreover, Lancaster et al. (Ref 7) reported that the soluble sulfur content in the weld pool can be calculated from the following:

$$S_{soluble} = S_{total} - 1.3Mg - 0.8Ca - 0.22(Ca + Ce) \quad \text{(Eq 1)}$$

The steels used in this study are free of magnesium, calcium, and cerium; consequently, the total sulfur content can be regarded as soluble. Figure 5 shows the effects of the phosphorus content in the base metal on the weld *d*/*w* ratio. It is clear that increased phosphorus content decreases the weld *d*/*w* ratio, but its effect was minor. In liquid iron, the surface-active intensity sequence of the nonmetallic elements (Ref 8) is as follows:

$$Te > Se \geq F > O \geq S > Sb > As \geq P > Si > C \geq B$$

Obviously, the surface-active intensity of phosphorus is far lower than the sulfur. On the other hand, although the increased phosphorus content can decrease the surface tension of the weld pool, the surface tension gradient is negative and hence decreases the weld *d*/*w* ratio. This phenomenon is different from the case in which the surface tension gradient is positive due to the addition of sulfur, because the FeP formed in the surface of the weld pool is more stable than FeS (Ref 8).

Figure 6 shows the relationship between silicon content of the base metal and the weld *d*/*w* ratio. The *d*/*w* ratio increases slightly with increasing silicon content, because the addition of silicon decreases the viscosity of the fluid in the weld pool, improves the fluidity, and consequently increases the weld *d*/*w* ratio (Ref 9). Figure 7 shows the effect of aluminum content on the *d*/*w* ratio. It is obvious that the addition of aluminum markedly decreases the weld *d*/*w* ratio. Full penetration can be made when the aluminum content of the base metal is lower than 60 ppm; however, the penetration is only half of the thickness when aluminum is above 60 ppm. Aluminum is not a surface-active element but a strong deoxidant, and it can significantly reduce the soluble oxygen content in the weld pool. The higher

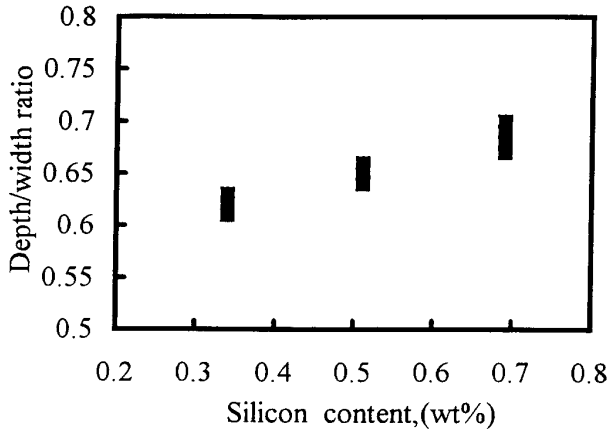

Fig. 6 Relationship between silicon content of the base metal and the weld *d*/*w* ratio

the aluminum content of the base metal, the lower the soluble oxygen content in the weld pool and, hence, the lower the weld *d*/*w* ratio (Ref 9).

Figure 8 shows the relationship between oxygen content of the base metal and the weld *d*/*w* ratio. It is clear that oxygen has a marked effect on the *d*/*w* ratio. When oxygen content is around 70 ppm, only one-third of thickness is penetrated; however, full penetration is reached at about 120 ppm. The surface tension gradient changes from negative to positive when the soluble oxygen content exceeds 40 ppm. In this case, the flow of the weld pool is inward and greatly increases the weld *d*/*w* ratio (Ref 6). There is no quantitative literature mentioning the relationship between soluble oxygen content in weld pool and deoxidants, such as aluminum, silicon, and manganese. Due to the strong affinity of aluminum to oxygen, and the fact that the melting point of Al_2O_3 can be as high as 2050 °C (Ref 10), which is higher than the temperature of the weld pool in the TIG welding of stainless steels (Ref 11), the soluble oxygen content in the weld pool seems expressible by the following equation without the addition of calcium and rare earth metal (REM) elements:

$$O_{soluble} = O_{total} - 0.89Al \quad \text{(Eq 2)}$$

Figure 9 shows the result of regression analysis for comparing the effect of elements on the weld *d*/*w* ratio. The effects of minor elements on the *d*/*w* ratio can be expressed by the following equation:

$$d/w \text{ ratio} = 0.2 + 57.2\,O - 36.2\,Al + 2.6\,S - 0.18\,P + 0.17\,Si \quad \text{(Eq 3)}$$

It is clear that the oxygen has a much greater effect on the weld penetration than sulfur does. A.M. Makara et al. (Ref 12) studied the effect of oxygen and sulfur content on the weld penetration of high-strength steels and suggest that the effect of oxygen is more significant than that of sulfur. In addition, it is the amount of soluble oxygen and sulfur in the weld pool that affects the weld penetration, not the total amount of these elements. The steels used in this study are free of magnesium, calcium, and cerium, which might combine with sulfur, and the soluble sulfur content in the weld pool is the same as the total sulfur content of base metal. However, the soluble oxygen content will be reduced by the addition of 50 to 90 ppm aluminum.

In addition, TIG butt welds were also performed between similar and dissimilar stainless steel heats to investigate the sulfur content on the effect of weld geometry. Figure 10 shows the cross-sectional view of the TIG butt welds. The formation of symmetrical weld is obtained due to the same sulfur content in the two metals (Fig. 10a). However, Fig. 10(b) demonstrates the formation of a nonsymmetrical weld geometry resulting from diffusocapillary and thermocapillary action due to different sulfur levels in two metals.

3.2 The Analysis of the Variation of Weld Geometry

Figure 11(a) shows the weld cross-sectional view of the O1 specimen (see Table 1) from a TIG bead-on-plate weld. There is considerable variation of weld geometry. Full penetration is reached (Fig. 11b) at narrower location of the weld in Fig. 11(a); however, only one-third of the thickness is penetrated at the wider weld (Fig. 11c). The variable weld penetration can occur even in the same stainless steel heats during mechanized

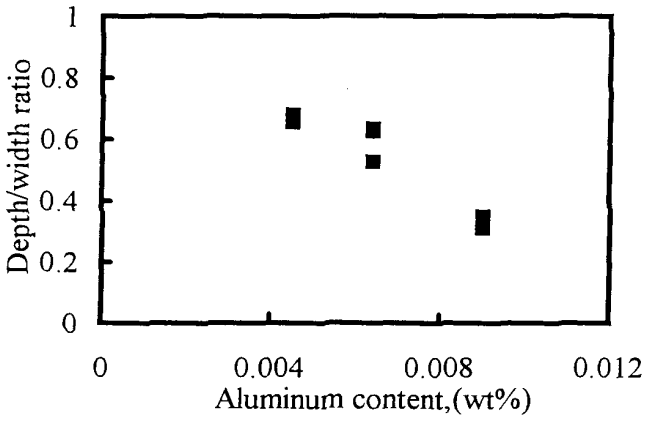

Fig. 7 Effect of aluminum content of base metal on the weld *d*/*w* ratio

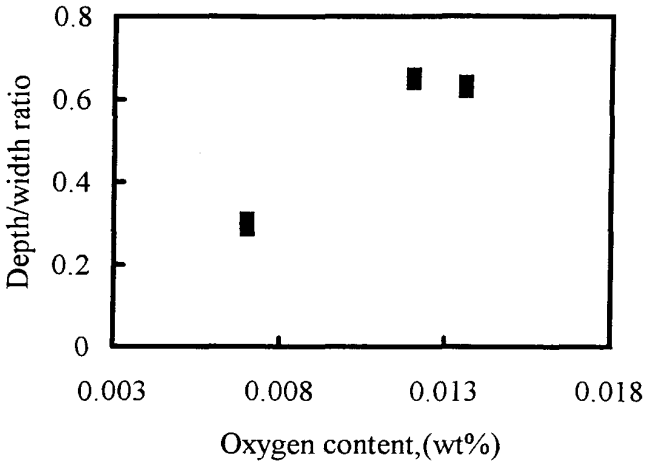

Fig. 8 Relationship between oxygen content and the weld *d*/*w* ratio

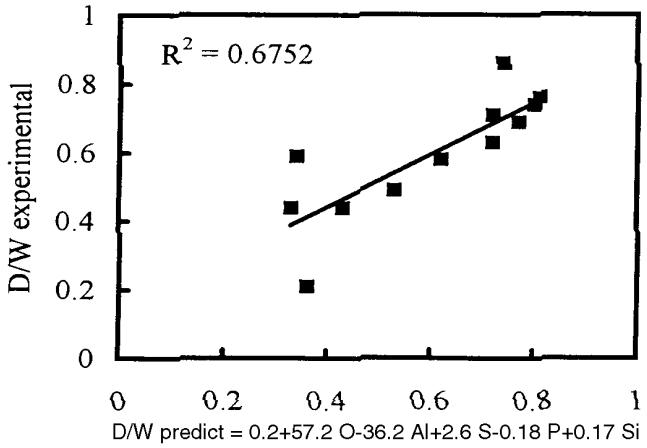

Fig. 9 Result of linear regression for comparing the effect of chemical composition on the weld *d*/*w* ratio

TIG welding. No research has been reported concerning the variation of weld geometry at the same weld. Figure 12 shows the microstructure of the full penetration weld of the O1 specimen which has many inclusion clusters. From SEM-EDS analysis, these oxide inclusions contain titanium, chromium, aluminum, and manganese. Table 3 lists the comparison of metallurgical characteristics for the variable TIG weld. Both the δ ferrite content and hardness are the same, irrespective of full or partial weld. It is implied that the variation of weld geometry at the same stainless steel heat does not result from the segregation of alloying elements and/or the change of the weld geometry. On the other hand, the volume fraction of inclusions in the full penetration weld is much higher than that of partial penetration weld (Table 3). According to these results, the variation of weld geometry at the same weld is related with the distribution of oxide inclusions owing to the O1 specimen having low sulfur content. In general, the solubility of oxygen in steel is very low, and it exists in the form of oxide.

During stainless steel TIG welding, the temperature in the weld pool is around 1600 °C (Ref 13), and the inclusions in the steel will be remelted (Ref 10) except for those with high melting points (e.g., Al_2O_3, 2050 °C; or REM-oxysulfide, >1800 °C). The remelting of low-melting-point oxides will increase the soluble oxygen content in the weld pool. The greater the distribution of low-melting-point oxide inclusions, the higher the soluble oxygen content in the weld pool is and vice versa, which results in the significant variation of weld geometry. To obtain a more consistent weld profile, the distribution of inclusions of the base metal should be as uniform as possible.

Table 3 The comparison of metallurgical characteristics for the variation of weld penetration obtained from O1 specimen during TIG bead-on-plate weld

Weld geometry	δ ferrite, %	Hardness, HV	Volume fraction of inclusion (10^{-3})	*d*/*w* ratio
Full penetration	4.0	184	1.17	0.7
Partial penetration	3.9	188	0.43	0.2

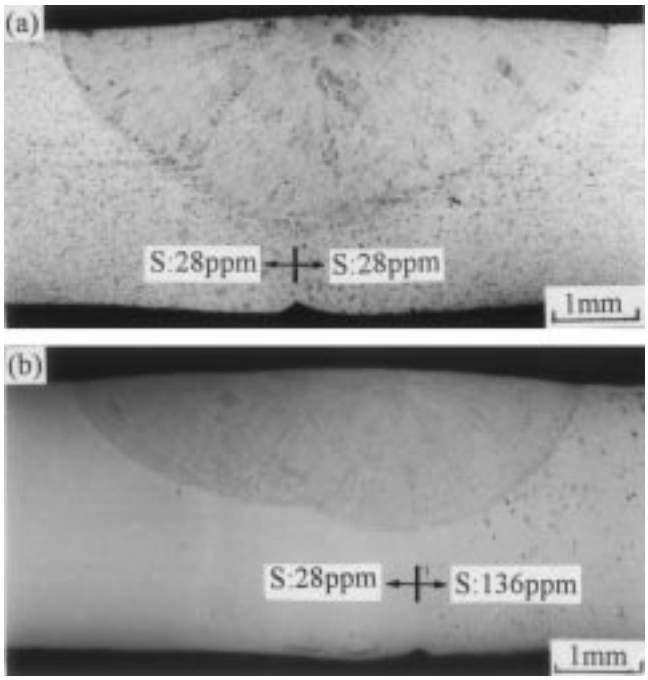

Fig. 10 Cross-sectional views obtained by welding steels with different sulfur contents during TIG butt welding

3.3 The Effect of Shielding Gas on the Weld Penetration

As previously discussed, the decreased oxygen and sulfur content will deteriorate the penetration of the weld. To improve the poor penetration characteristics of high-purity type 304 stainless steel, small amounts of O_2 or H_2 gas are added into the argon torch shielding gas (Ref 14). Figure 13 shows the effect of shielding gas on the weld *d*/*w* ratio. It is clear that the weld *d*/*w* ratio is lowest when pure argon is used. Conversely, the weld *d*/*w* ratio could be markedly promoted with the introduction of 1% O_2 or 5% H_2 into the argon-base shielding gas. This improvement is possible because the soluble oxygen content in the weld pool is increased, which improves weld penetration. However, due to high-temperature oxidation, the electrode life will greatly deteriorate when a small amount of oxygen is added into the shielding gas. On the other hand, in the case of

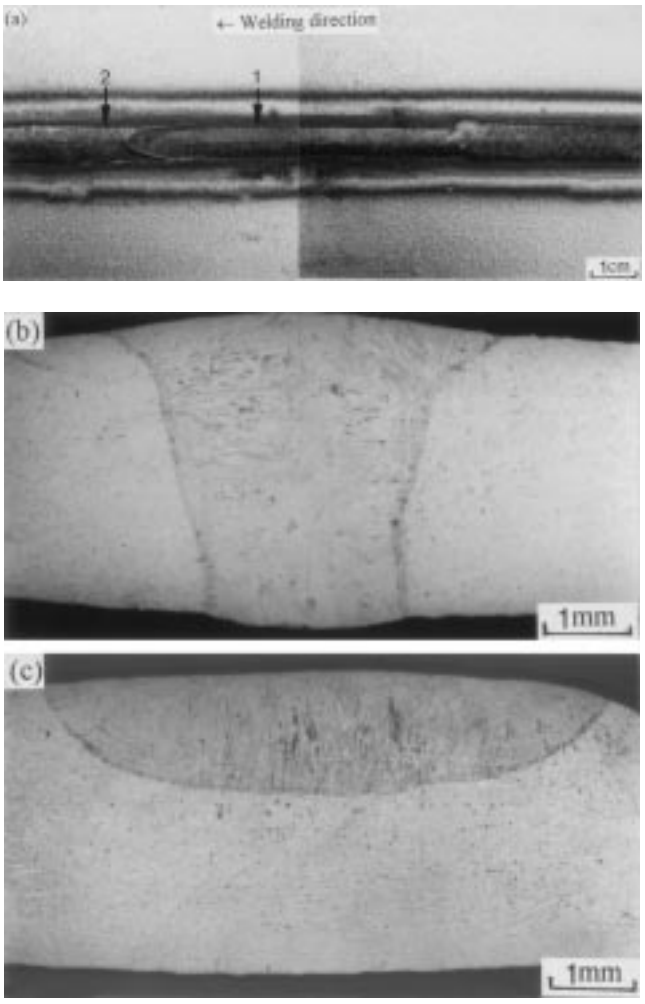

Fig. 11 (a) Weld appearance of O1 specimen from TIG bead-on-plate weld. (b) Cross section of position 1. (c) Cross section of position 2

Ar + 5% H_2, the improvement in the *d*/*w* ratio is attributed to the high thermal conductivity of hydrogen and gives a larger heat input (Ref 15). In addition, the usage of Ar + 1% O_2 or Ar + 5% H_2 shielding gas reaches full penetration even though the sulfur content of steel is only 30 ppm, but the latter produces the wider weld and, hence, slightly reduces the weld *d*/*w* ratio. Consequently, hydrogen affects the weld depth more than it affects the width. Moreover, Fig. 13 also shows that the weld *d*/*w* ratio increases with increasing sulfur content of the base metal when Ar and Ar + H_2 are used. On the other hand, the weld *d*/*w* ratio reaches saturation at about 70 ppm sulfur content for Ar + H_2. However, it decreases with increasing sulfur content when Ar + 1% O_2 is utilized. This phenomenon is different from the expectation that the increased oxygen and sulfur content simultaneously can promote the weld *d*/*w* ratio. The kinetics of oxygen dissolution might be affected by the nature of the weld pool surface, and the sulfur occupation of the surface may inhibit oxygen dissolution (Ref 11). Therefore, when the sulfur content of the weld pool increases, the soluble oxygen content in the weld pool will decrease, and the weld *d*/*w* ratio will be reduced.

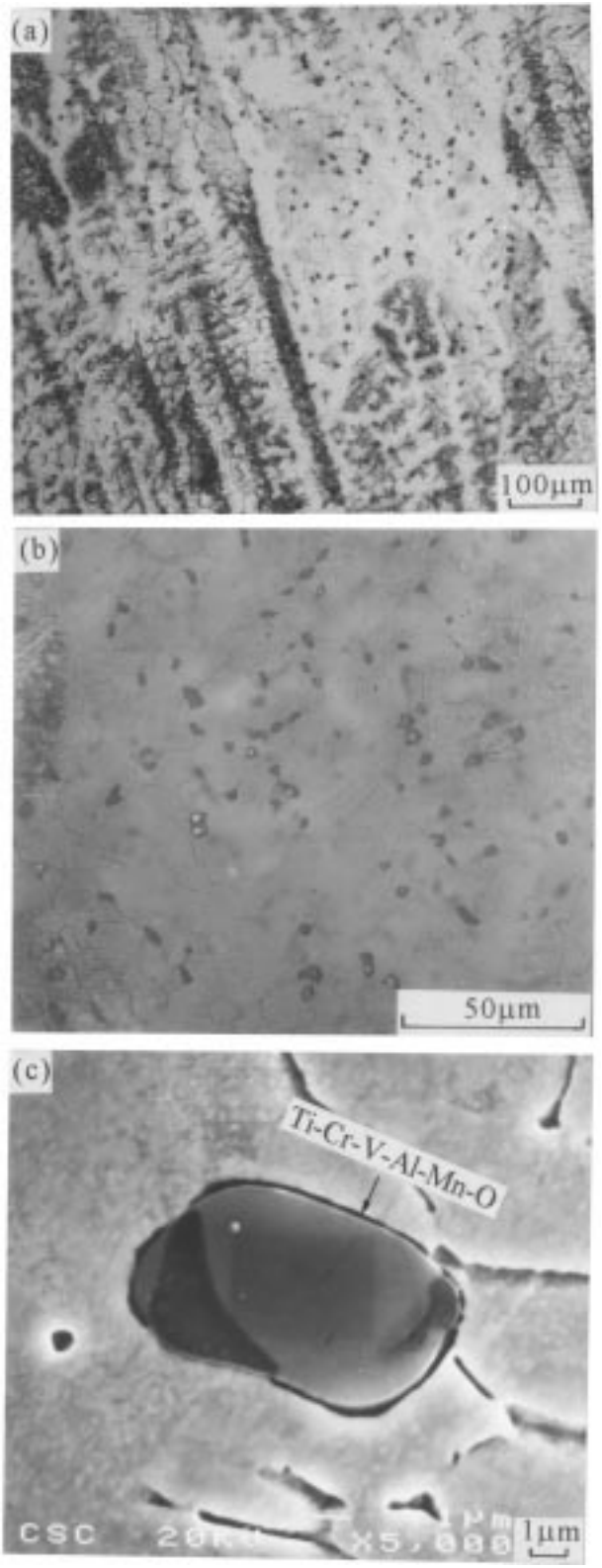

Fig. 12 Micrograph of full penetration weld of O1 specimen from bead-on-plate weld. (a) and (b) OM. (c) SEM

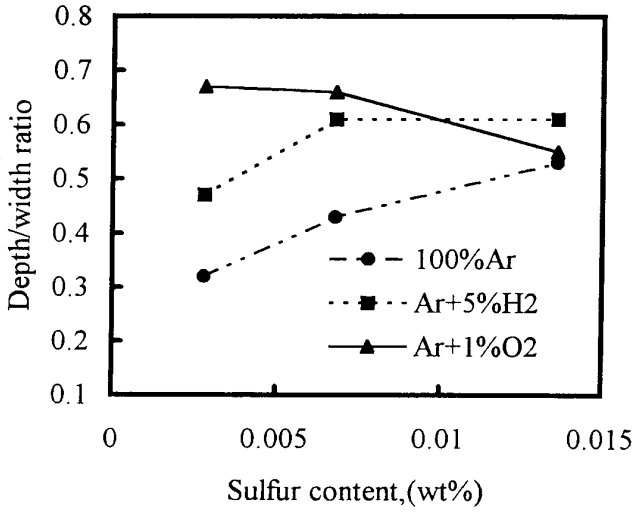

Fig. 13 The effect of shielding gas on the weld *d*/*w* ratio at a variety of sulfur contents

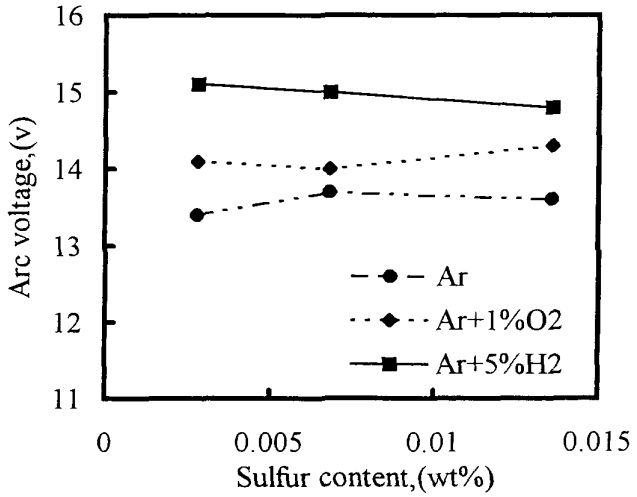

Fig. 14 The effect of shielding gas on the arc voltage at a variety of sulfur contents

Figure 14 shows the relationship between the shielding gas and the arc voltage. For a constant arc length, the arc voltage for Ar + 5% H_2 is approximately 15 V at a 150 A welding current, which is 1.5 V higher than that of pure argon. This increase in arc voltage with the addition of 5% H_2 into the argon-base shielding gas can be attributed to an increase in electrical field strength due to the higher thermal conductivity of H_2 compared to that of argon (Ref 15). On the other hand, the addition of 1% O_2 into the shielding gas also increases arc voltage about 0.5 V compared to that of argon gas. The higher the arc voltage is, the wider the weld width is; therefore, the width of the weld using Ar + 5% H_2 is wider than that when Ar + 1% O_2 or pure argon is used. In addition, Fig. 14 shows how the increased sulfur content has no effect on the arc voltage. This result agrees with those reported by Lambert (Ref 16). Because hydrogen influences the weld depth more than it influences the width, the effect of the addition of H_2 on the weld *d*/*w* ratio is still higher than pure argon. The addition of H_2 to an argon-base shielding gas increases the heat input by altering the heat generating process in the arc rather than altering the weld pool fluid-flow behavior as suggested by a Maragoni fluid-flow mode (Ref 5). However, the addition of oxygen increases the soluble oxygen content in the weld pool and changes the surface tension gradient from negative to positive and, hence, promotes the weld *d*/*w* ratio.

4. Summary and Conclusions

During the development of type 304 stainless steel, variable penetration is present during mechanized TIG welding. From the bead-on-plate test and the analysis of the metallurgical characteristics of the weld, these main conclusions were drawn:

- The minor elements, such as oxygen, aluminum, and sulfur, have a significant effect on the weld *d*/*w* ratio. The increased oxygen and sulfur content promotes the weld *d*/*w* ratio. However, aluminum has a strong affinity to oxygen and decreases the soluble oxygen content in the weld pool, which markedly decreases the weld *d*/*w* ratio. In addition, the effect of silicon and phosphorus on the weld *d*/*w* ratio is insignificant. The effects of the minor elements on the *d*/*w* ratio with linear regression are summarized:

$$d/w \text{ ratio} = 0.2 + 57.2O - 36.2Al + 2.6S - 0.18P + 0.17Si$$

- The formation of a nonsymmetrical weld geometry with different sulfur content during TIG butt welding is a result of the diffusocapillary and thermocapillary action.
- The distribution of inclusions in the base metal has a marked effect on the weld geometry during mechanized TIG bead-on-plate weld. The distribution of inclusions in the base metal should be as uniform as possible to obtain a more consistent weld profile.
- The addition of 1% O_2 or 5% H_2 to the argon-base shielding gas greatly promotes the weld *d*/*w* ratio. The former is due to the increased soluble content in the weld pool, and the latter is because of the production of a hotter arc than that produced by pure argon.

References

1. G.W. Olyer, R.A. Matsuzesk, and C.R. Garr, *Weld. J.*, Vol 46, 1967, p 1006
2. K.J. Rodgers, "The Effects of Residual Impurity and Microalloying Elements on Weldability and Weld Properties," paper 2, The Welding Institute, Abington, U.K., 1983
3. D.K. Aidum and S.A. Martin, *J. Mater. Eng. Perform.*, Vol 60, 1997, p 496
4. B.J. Keene, K.C. Mill, and R.F. Brooks, *J. Mater. Sci. Technol.*, Vol 1, 1985, p 568
5. C.R. Heiple, J.R. Roper, R.T. Stagner, and R.J. Aden, *Weld. J.*, Vol 62, 1983, p 72s
6. K.C. Mill and B.J. Keene, *Int. Mater. Rev.*, Vol 35, 1990, p 185
7. J.F. Lancaster and K.C. Mills, International Institute of Welding recommendation 212-796-91
8. X.M. Xue, H.G. Jiang, Z.T. Sui, B.Z. Ding, and Z.Q. Hu, *Metall. Trans. B*, Vol 27, 1996, p 71
9. B. Pollard, *Weld. J.*, Vol 67, 1988, p 202s
10. J.M. Dowling, J.M. Corbett, and H.W. Kerr, *Metall.Trans. A*, Vol 17, 1986, p 1611
11. J.F. Lancaster, *The Physics of Welding*, 2nd ed., International Institute of Welding, 1986
12. A.M. Makara, *Automat. Weld.*, Vol 9, 1977, p 1
13. H. Kokawa, J. Okada, and T. Kuwana, *Q. J. Jpn. Weld. Soc.*, Vol 10, 1992, p 496
14. J.A. Lambert, *Weld. J.*, Vol 67, 1988, p 202s
15. M. Onien, R. Peters, D.L. Olson, and S. Liu, *Weld. J.*, Vol 74, 1995, p 10s
16. J.A. Lambert, *Weld. J.*, Vol 70, 1991, p 41